NEMS-based optical phase modulator fabricated on Silicon-On-Insulator

Karel Van Acoleyen, Joris Roels, Tom Claes, Dries Van Thourhout and Roel Baets
Photonics Research Group
Department of Information Technology (INTEC)
Ghent University - imec, Belgium
Email: karel.vanacoleyen@intec.ugent.be

***Abstract*—We present a compact low-power optical phase modulator on Silicon-On-Insulator consisting of an under-etched slot waveguide. By applying a voltage of 15V across a 9μm long slot waveguide an optical phase change of 60° was observed.**

I. Introduction

Optical phase modulation is of great interest in data modulation or tuning applications. Using the CMOS (Complementary Metal Oxide Semiconductor) compatible silicon photonics platform, several approaches have been undertaken. The easiest and simplest approach of phase modulation is using the thermo-optic effect in silicon. This effect is rather large in silicon but still has a relatively large power consumption due the continuous current flow. Furthermore, the speed is limited as the thermo-optic response is in the μs range [1], [2]. Carrier based modulators on the other hand are capable to reach up to ten Gbps and higher, but are relatively large and lossy as the carriers increase the optical absorption of the waveguides [3]. In this paper we present a compact, low-power optical phase modulator technique based on nanoelectromechanical systems (NEMS) using an under-etched slot waveguide.

Apart from its attractive optical properties, crystalline silicon also has good mechanical properties. This stimulated a rapid development of this field in fabricating ultra sensitive sensors [4]. This platform furthermore allowed to observe and measure optical forces [5]. The principle of using a free-standing slot waveguide as phase modulator was already explained in [6], but here we present to our knowledge the first experimental demonstration. When a voltage is applied across a free-standing slot waveguide, the slot spacing will change resulting in an effective index change and thus a phase change. As there is no current flowing through the system, only power is consumed when switching.

Next we discuss the design and fabrication of the component. In Section III a mathematical description is given. Section IV gives the measurement results. A conclusion is finally formulated in Section V.

II. Design and Fabrication

The principle of phase modulation is based on the fact that the effective index of a slot waveguide will change by changing the slot spacing. The effective index of the fundamental TE-like mode of the slot waveguide (Fig. 1) was calculated using the Fimmwave mode solver and can be found

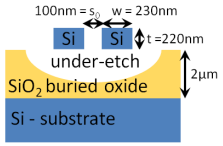

Fig. 1. Cross section of the under-etched slot waveguide.

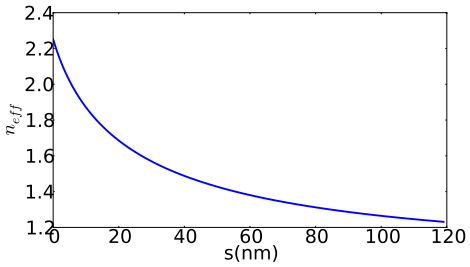

Fig. 2. Effective index of the fundamental TE-like mode of the slot as a function of slot spacing at a wavelength of 1550nm.

in Fig. 2. A large change in effective index occurs as the spacing becomes smaller. The spacing of the slot is changed by under-etching the slot waveguide and applying a voltage across the slot. By increasing the voltage, the beams are attracted and the spacing becomes smaller. This increases the attractive force even more. At a certain point, the attractive force becomes too large for the slot to be countered by the elastic force and the system becomes unstable resulting in a collapse of the slot waveguide. This is known as the 'pull-in' effect in the MEMS (MicroElectroMechanical Systems) world and as a general rule of thumb occurs when the spacing is less than one third of the nominal spacing. The slot waveguide is placed in a Fabry-Pérot cavity which allows us to measure the phase change by means of a spectral shift of the resonant wavelengths.

The component shown in Fig. 3 was fabricated on Silicon-On-Insulator (SOI) at *imec*, using standard CMOS (Complementary Metal Oxide Semiconductor) compatible processes [7] on an SOI wafer with a 2μm buried oxide layer and a 220nm silicon top layer. An etch of 220nm was used to etch the waveguides and slot waveguide, while the Bragg mirrors were defined with a 70nm etch. Light is guided from an optical fiber into the structure using a grating coupler for near vertical

978-1-4244-8339-6/11/$26.00 ©2011 IEEE

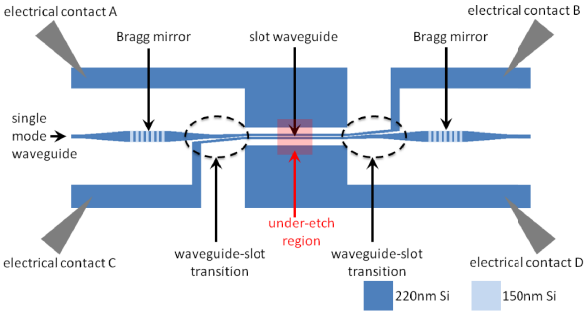

(a)

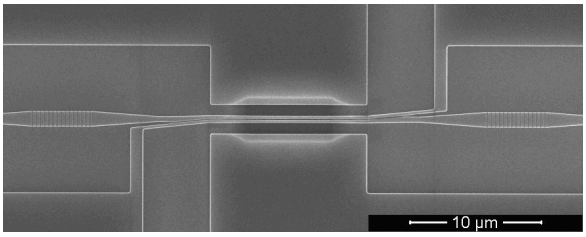

(b)

Fig. 3. (a) Schematic of the NEMS based phase modulator (b) SEM picture.

coupling of the TE-like mode [8]. The waveguide is then adiabatically tapered to a 450nm wide photonic wire which is the input waveguide shown in Fig. 3(a). Light enters into the Fabry-Pérot cavity where a waveguide-slot transition excites the slot waveguide. Finally the slot waveguide tapers back to a single mode waveguide and to an optical fiber, again through a grating coupler. The slot waveguide consists of 230nm wide beams with a slot spacing of 100nm (Fig. 1). Afterward the slot waveguide is under-etched. This is done by defining an etch region using contact-mask lithography and etching the buried oxide with buffered HF (hydrofluoric acid) for about 8 minutes. Fig. 3(b) shows a SEM (Scanning Electron Microscope) picture of the final component. The slot waveguide is free-standing over a length of $L = 9\mu\text{m}$. A voltage is applied across the electrical contacts B and C to attract the beams of the slot waveguide. The other contacts can be used to repel the beams.

III. Mathematical Description

The movement $a(x)$ of the beams of the slot can be described by the Euler beam equation, where the residual axial stress is neglected in first instance:

$$EI\frac{\mathrm{d}^4 a}{\mathrm{d}x^4} = p(x) \tag{1}$$

Where E is Young's modulus (= 169GPa in Si for the crystallographic direction of interest), $p(x)$ is the force distribution along the beam and I is the beam's area moment of inertia, defined as:

$$I = \frac{wt^3}{12} \tag{2}$$

with w and t the width and thickness of the beam, respectively. When a voltage is applied across the slot, a force will be exerted on both beams which will depend on the spacing of the slot waveguide. The force distribution $p(x)$ (N/m) can be expressed as:

$$p(x) = \frac{1}{2}V^2\frac{\partial C(s(x))}{\partial s(x)}, \tag{3}$$

where V is the applied voltage and $C(s(x))$ is the capacitance distribution (F/m) across the slot, which is a function of $s(x)$, the spacing of the slot. The capacitance distribution is given by:

$$C(x) = \epsilon_0\frac{t}{s(x)}, \tag{4}$$

The magnitude of the force distribution is then given by:

$$p(x) = \frac{1}{2}V^2\frac{\epsilon_0 t}{s(x)^2}, \tag{5}$$

with ϵ_0 the vacuum permittivity. There is a squared dependence on the applied voltage and on the spacing. This spacing between the slots is dependent on the beam excursion $a(x)$ as:

$$s(x) = s_0 - 2a(x), \tag{6}$$

where s_0 is the slot spacing when no voltage is applied. The force term $p(x)$ in (1) is thus a function of $a(x)$ and makes this a nonlinear differential equation. Fixed boundary conditions are assumed at the clamping points $x = 0$ and $x = L$ allowing no displacement or rotation:

$$a = 0; \frac{\mathrm{d}a}{\mathrm{d}x} = 0 \tag{7}$$

This equation is solved numerically using the parameters given in Section II. In Fig. 4, the beam excursion of one of the slot beams is shown as a function of x for different voltages. When the voltage becomes larger than the 'pull-in' voltage, the system becomes unstable and no solution is found. A stable solution was found up to an applied voltage of 18V.

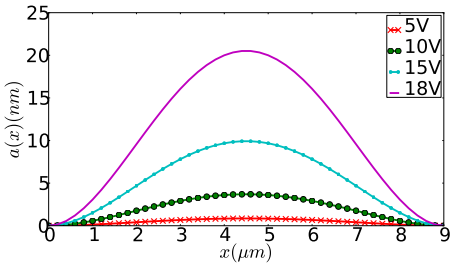

Fig. 4. Beam excursion of one of the beams as a function of x for different applied voltages.

Knowing the beam excursion, the effective index change of the complete slot (Fig. 2) can be calculated. This results in a phase change $\Delta\phi$. Fig. 5 shows the expected phase change until 'pull-in' occurs for different lengths of the under-etched slot at $\lambda = 1550$nm. When L becomes larger, a big increase of the effect can be seen, as there is a bigger effective index change and the beams become more elastic. While for a $10\mu\text{m}$ length a π phase difference can not be obtained, this is already

possible for a 15µm length. The important figure of merit $V_\pi L_\pi$ is 96Vµm, 68Vµm and 52.5Vµm for a length of 15µm, 20µm and 25µm, respectively. While longer modulators have an increased figure of merit, they will be inherently slower as the mechanical relaxation constants will increase.

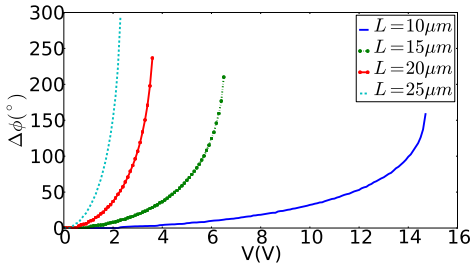

Fig. 5. Theoretically predicted phase change as a function of applied voltage across the slot for different lengths L. The curves are drawn up to the point where 'pull-in' occurs.

IV. Measurement Results

We measured the Fabry-Pérot spectrum by exciting the structure with a broadband superluminescent LED (Light Emitting Diode) and measuring the transmission using an Optical Spectrum Analyzer (OSA). The spectra are shown in Fig. 6. The Bragg mirrors were relatively weak which results in broad resonances. The insertion loss at the Fabry-Pérot resonance near 1525nm is about 5dB. For larger wavelengths, the transmission decreases which suggests that the slot mode is reaching cut-off. By measuring the peak shift for different voltages, the effective phase change inside the slot can be calculated. This is shown in Fig. 7, where also the theoretical solution is shown. A good agreement can be seen. We note that the actual result is very dependent on the actual under-etch length (see Fig. 5) and the initial spacing of the slot s_0. The difference between theoretical and experimental phase change may be explained by the residual axial stress when the deformation becomes larger, but requires further investigation. The dynamic behavior is currently under investigation.

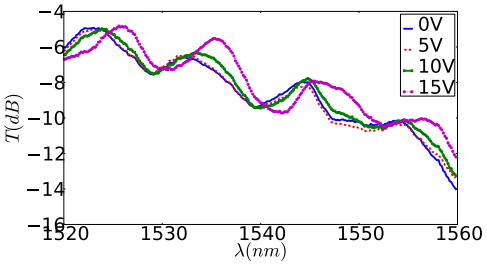

Fig. 6. Measured Fabry-Pérot spectrum of the slot waveguide for different applied voltages.

V. Conclusion

A low-power NEMS based phase modulator has been fabricated and measured. The component consists of an under-etched slot waveguide in SOI. Phase changes of 60° have been measured for a length of $L = 9\mu m$ and an applied voltage of 15V. Increasing this length will greatly improve these characteristics by lowering the operation voltage and increasing the phase change. This will however reduce the speed of the component as a large mechanical resonator has a longer relaxation time. By cascading several short under-etched waveguides, the effect can be increased without compromising the speed.

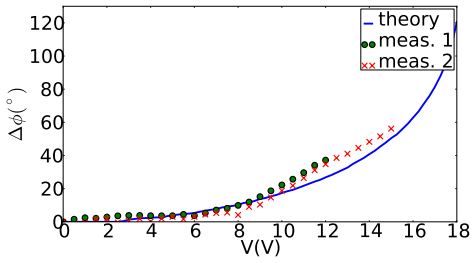

Fig. 7. Theoretically predicted and measured phase change as a function of applied voltage across the slot for two different measurements (meas. 1 and meas. 2).

Acknowledgment

Karel Van Acoleyen acknowledges the Research Foundation - Flanders (FWO) for a research grant. This work was supported by the Methusalem project Smart Photonic ICs of Ghent University and the IAP project Photonics@be. The authors would like to thank Bram De Geyter for the help in the design of the component and Liesbet Van Landschoot and Steven Verstuyft for the help in the post-processing.

References

[1] R. L. Espinola, M. C. Tsai, J. T. Yardley, and R. M. Osgood, "Fast and low-power thermooptic switch on thin silicon-on-insulator," *IEEE Photonics Technology Letters*, vol. 15, no. 10, pp. 1366–1368, 2003.

[2] J. Van Campenhout, W. M. J. Green, S. Assefa, and Y. A. Vlasov, "Integrated NiSi waveguide heaters for CMOS-compatible silicon thermo-optic devices," *Optics Letters*, vol. 35, no. 7, pp. 1013–1015, 2010.

[3] N. N. Feng, S. R. Liao, D. Z. Feng, P. Dong, D. W. Zheng, H. Liang, R. Shafiiha, G. L. Li, J. E. Cunningham, A. V. Krishnamoorthy, and M. Asghari, "High speed carrier-depletion modulators with 1.4V-cm V pi L integrated on 0.25 mu m silicon-on-insulator waveguides," *Optics Express*, vol. 18, no. 8, pp. 7994–7999, 2010.

[4] I. De Vlaminck, J. Roels, D. Taillaert, D. Van Thourhout, R. Baets, L. Lagae, and G. Borghs, "Detection of nanomechanical motion by evanescent light wave coupling," *Applied Physics Letters*, vol. 90, no. 23, p. 3, 2007.

[5] J. Roels, I. De Vlaminck, L. Lagae, B. Maes, D. Van Thourhout, and R. Baets, "Tunable optical forces between nanophotonic waveguides," *Nature Nanotechnology*, vol. 4, no. 8, pp. 510–513, 2009.

[6] V. R. Almeida and R. R. Panepucci, "NOEMS devices based on Slot-Waveguides," in *2007 Conference on Lasers & Electro-Optics/Quantum Electronics and Laser Science Conference*, Baltimore, 2007.

[7] ePIXfab, "The silicon photonics platform," *http://www.epixfab.eu/*, 2011.

[8] D. Vermeulen, S. Selvaraja, G. Verheyen, P. Lepage, W. Bogaerts, and G. Roelkens, "High-efficiency Silicon-On-Insulator Fiber-to-Chip Grating Couplers Using a Silicon Overlay," in *Group IV Photonics*, United States, 2009, p. FPd1.